Supplementary materials

Supplementary Figure 1.

(**A**) **Effects of EGF stimulation on actin organization in A431 cells.** Immunofluorescence analyses of endogenous F-actin localization. Cells were incubated for 1 h in serum-free Ringer's buffer, and 8 min in Ringer's buffer in the absence (w/o) and presence (+) of 50 ng/ml EGF. The cells were then fixed and stained with 488-conjugated phalloidin to reveal actin organization. (**B**) **Inhibition of EGF-stimulated macropinocytosis in A431 cells.** Cells were incubated for 1 h in serum-free Ringer's buffer, and then 8 min in Ringer's buffer containing 50 ng/ml EGF and TRITC-conjugated dextran. The cells were also pre-treated with the following inhibitors: 200 μM amiloride (*vs*. Na^+/H^+ echanger), 5 min; 5 μg/ml cytochalasin D (actin depolymerising drug), 10 min; 100 nM wortmannin (*vs*. PI 3-kinases, PI3k), 15 min; 10 μM Ro31-8220 (*vs*. protein kinase C, PKC), 10 min; 10 μM Go-6976 (*vs*. protein kinase C, PKC), 10 min; 20 μM BAPTA (Ca^{2+} chelator), 30 min, 10 μM U73343 (*vs*. phospholipase C, PLC), 10 min. After fixing, the cells were examined under confocal microscopy for macropinocytosis (see Methods). (**C**) **CtBP1/BARS levels in siRNAs-treated A431 cells.** Cells were transfected for 72 h with non-targeting siRNAs or siRNAs targeted to CtBP1/BARS. Each lane contains the same amount of total protein (not shown). (**D**) **Effects on actin organization of siRNAs targeted to CtBP1/BARS in A431 cells.** Cells were transfected as for **C**, incubated for 1 h in serum-free Ringer's buffer, and 8 min in Ringer's buffer with 50 ng/ml EGF. The cells were then fixed and stained with 488-conjugated phalloidin to reveal actin organization. (**E**) **Effects of long exposures to high levels of cytosolic CtBP1/BARS in A431 cells.** Cells were transfected with YFP or CtBP1/BARS-YFP, or microinjected with GST or CtBP1/BARS-GST, and 24 h later they were incubated for 1 h in serum-free Ringer's buffer, and 8 min in Ringer's buffer with 50 ng/ml EGF. After fixing, the cells were examined under confocal microscopy for macropinocytosis. More than 100 cells were analyzed under each experimental condition, and data are means ±S.D. from three independent experiments. Scale bars: A, 10 μm; D, 30 μm.

Supplementary Figure 2.

(A) Pak1-mediated *in-vitro* phosphorylation of CtBP1-S/BARS. Purified recombinant Pak1 (0.1 µg) was incubated with 4 µg CtBP1/BARS or 4 µg cortactin in HEPES buffer containing 25 µM ATP and 0.8 µCi [^{32}P]-ATP. Samples were run on SDS-PAGE and analysed by electronic autoradiography (Instant Imager, Packard). (**B**) **CtBP1/BARS is phosphorylated during EGF stimulation in A431 cells**. Cells were incubated for 1 h in serum-free Ringer's buffer, and 8 min in Ringer's buffer in the absence (-) or presence (+) of 50 ng/ml EGF. CtBP1/BARS was then immuno-precipitated from total cell lysates (prepared with RIPA buffer). The level of CtBP1/BARS phosphorylation was assessed with an anti-phosphoserine antibody (Ab), while the total CtBP1/BARS immuno-precipitated was assessed with a monoclonal anti-CtBP1/BARS antibody. (**C**) **Localization of CtBP1/BARS mutants in non-stimulated A431 cells.** Immunofluorescence analyses of wild-type (wt) CtBP/BARS and its S147A and S147D mutants, and of F-actin localization. Cells were transfected for 6 h with the indicated constructs, and incubated for 1 h in serum-free Ringer's buffer. The cells were then fixed and stained with the p50-2 anti-CtBP1/BARS antibody (CtBP1/BARS Ab; green), 546-conjugated phalloidin to reveal actin organization (F-actin; red), and tropo3-6333 as nucleus marker (blue); the merged signal is also shown. Scale bar, 10 µm. More than 100 cells were analyzed under each experimental condition.

Supplementary Figure 3. Crystal structure of the CtBP1/BARS dimer complex with the phosphorylated Ser147 highlighted in orange. (A) Ribbon representation and **(B, C)** a surface representation of the three-dimensional structure of CtBP1/BARS. Monomer 1 is in green, monomer 2 is in blue, and the phosphorylated serine is highlighted in orange. **(C)** A snapshot after 10 ns of molecular dynamics simulation from (B). Note in (C, arrowheads) that the SBD of monomer 1 (green) is partially detached from the loop containing the phosphorylation site (orange) of monomer 2 (blue), thereby reducing the stability of the complex.

Movie 1: CtBP1/BARS-YFP recruitment to plasma-membrane ruffles and the macropinocytic cup in A431 cells. Cells were transfected with CtBP1/BARS-YFP (6 h of over-expression), and incubated for 1 h in serum-free Ringer's buffer. During the acquisition of the movie, 50 ng/ml EGF and TRITC dextran were added. Time-lapse

imaging for CtBP1-S/BARS-YFP (green) and TRITC-dextran (red). In this movie, we can follow the recruitment of CtBP1/BARS to plasma-membrane ruffles and the macropinocytic cup. The large round macropinosomes that form from these cups then move rapidly into the cell (confirming the macropinocytic nature of the cups). CtBP1/BARS localization at the macropinocytic cup is transient, lasting only until the closure of the macropinosome.

Movie 2: CtBP1/BARS-YFP recruitment to plasma-membrane ruffles and the macropinocytic cup in A431 cells. Detail from Movie 1.

Movie 3: NBD-YFP recruitment to plasma-membrane ruffles and the macropinocytic cup in A431 cells. As for Movie 1, but with NBD-YFP transfection. Time-lapse imaging for NBD-YFP (green) and TRITC-dextran (red). In this movie, we can follow recruitment of NBD-YFP to plasma-membrane ruffles and the macropinocytic cup. However, these cups did not develop into macropinosomes, but are instead 'aborted' into a normal plasma-membrane ruffles.

Movie 4: NBD-YFP recruitment onto plasma membrane ruffles and the macropinocytic cup in A431 cells. Detail from Movie 3.

Supplementary methods

Binding analysis

To determine the role of CtBP1/BARS in membrane fissioning, we investigated the effects of Pak1 phosphorylation of CtBP1/BARS on the stability of its dimerisation. This loss of stability of the CtBP1/BARS dimer was suggested as the CtBP1/BARS phosphorylation site, Ser147, is located on the dimerisation interface, while also being accessible to enzyme activities (see Supplementary Figure 2). We have analysed 'snapshots' taken from the molecular dynamics simulations of the non-phosphorylated and phosphorylated dimers, and we see that phosphorylation decreases the free energy of binding of the CtBP1/BARS monomers by 84 (±33) kJ/mol. This weakening is mainly caused by electrostatic repulsion between the loop containing the phosphorylation site (_B – loop – _C) and the SBD of the second

monomer. This destabilisation is accompanied by increased internal fluctuations of the monomers, and especially of the SBDs (+14%). These results give a strong indication that Pak1-dependent phosphorylation of CtBP1/BARS can influence the oligomerization of CtBP1/BARS, shifting it towards the monomeric state.

Methods

The influence of this phosphorylation on the free energy of binding of two CtBP1/BARS monomers was estimated by differences in the free energies of binding between the phosphorylated and the non-phosphorylated dimer complexes ($\Delta\Delta G_{bind}$), as determined by the combined Molecular Mechanics/ Poisson-Boltzmann Surface Area approach[1]. To take account of the conformational flexibility of these CtBP1/BARS complexes and of possible conformational changes upon phosphorylation, the free energies of binding (ΔG_{bind}) for each of the CtBP1/BARS complexes were averaged over snapshots of molecular dynamics simulation trajectories:

$$\Delta\langle\Delta G_{bind}\rangle = \Delta\langle\Delta G_{MM}\rangle + \Delta\langle\Delta G_{solv}\rangle \_ T \cdot \Delta\langle\Delta S\rangle.$$

The solvation free energy $\Delta G_{solv} = \Delta G_{elec} + \Delta G_{nonpolar}$ was approximated as the sum of the electrostatic contributions that solve the linear Poisson-Boltzmann equation, plus a non-polar term. The latter was chosen as linearly dependent on the solvent-accessible surface A[2]:

$$\Delta G_{nonpolar} = \_ \cdot A + \_,$$

where _ = 0.00542 kcal/mol and _ = 0.92 kcal/mol. The Poisson-Boltzmann equation was numerically solved applying the DELPHI II programme[3], using an ionic strength of 0.1 M and a surface probe radius of 1.4 Å, a 245-cubed grid, and at a grid resolution of 2.5 grid points per Å. The interior, protein dielectric constant was chosen as $\varepsilon_i = 2$, and the exterior, water dielectric constant was set to $\varepsilon_e = 80$.

For the calculations of free energy of binding, no cut-offs for the Coulomb interaction or for the van der Waals interactions were applied. The structures of the complex and of the individual monomers were both extracted from the simulation of the complexes. Contributions due to the adaptation free energy[4] between the bound

and the free states of the CtBP1/BARS monomers, as well as the entropic contributions $_T\Delta S$, were assumed to be equal for the phosphorylated and the non-phosphorylated states.

These molecular dynamics simulations of the CtBP1/BARS dimer complexes were performed using the GROMACS software package[5] and the Gromos 53A6 forcefield[6]. The non-phosphorylated dimer complex was taken from the Protein Data Bank (PDB entry 1HL3 at 3.1 Å resolution[7]). To build the phosphorylated CtBP1/BARS dimer complex, Ser147 was manually replaced with phosphoserine on both monomers. The complexes were solvated with SPC water molecules[8], and with Na^+Cl^- ions at physiological concentrations. Electrostatic interactions were calculated using the Particle Mesh Ewald (PME) method[9]. An integration time step of 2 fs was applied. The temperature was kept constant at 310 °K by coupling the system to an external thermal bath[10]. All of the equilibrium molecular dynamics simulations were preceded by 200 steps of energy minimization using a steepest descent algorithm, followed by 100 ps of molecular dynamics simulation with harmonic position restraints (force constant, 1,000 kJ/mol/nm^2) on all of the heavy atoms of the protein. The total simulation length was 10 ns for each simulation.

Snapshots for the analyses of the free energies of binding were extracted from the molecular dynamics trajectories every 10 ps. The free energies of binding were computed for the final 5 ns of the simulation, after equilibration of the initial complex structures. The more unfavourable van der Waals interaction energy between the CtBP1/BARS monomers for the phosphorylated dimer contributed approximately 53 kJ/mol to the difference in binding energies, while the electrostatic free-energy contributions destabilize the phosphorylated dimer by 31 kJ/mol, with respect to the non-phosphorylated dimer.

References

1. P.A. Kollman, I. Massova, C. Reyes, B. Kuhn, S. Huo, L. Chong, M. Lee, T. Lee, Y. Duan, W. Wang, O. Donini, P. Cieplak, J. Srinivasan, D.A. Case, and T. E. Cheatham. Calculating structures and free energies of complex molecules: combining molecular mechanics and continuum methods. 2000. *Acc. Chem. Res*. 33, 889–897.
2. D. Sitkoff, K. A. Sharp, and B. Honig. Accurate calculation of hydration free energies using macroscopic solvent models. 1994. *J. Phys. Chem*. 98,

1978–1988.

3. W. Rocchia, E. Alexov, and B. Honig. Extending the applicability of the non-linear Poisson-Boltzmann Equation: multiple dielectric constants and multivalent ions. 2001. *J. Phys. Chem. B* 105, 6507–6514.
4. C.M. Reyes and P.A. Kollman. Structure and thermodynamics of RNA-protein binding: using molecular dynamics and free energy analyses to calculate the free energies of binding and conformational change. 2000. *J. Molec. Biol.* 297, 1145–1158.
5. D. van der Spoel, E. Lindahl, B. Hess, G. Groenhof, A. E. Mark, and H. J. C. Berendsen. GROMACS: fast, flexible and free. 2005. *J. Comp. Chem*. 26, 1701–1718.
6. C. Oostenbrink, A. Villa, A.E. Mark, and W. F. van Gunsteren. A biomolecular force field based on the free enthalpy of hydration and solvation: the GROMOS force-field parameter sets 53A5 and 53A6. 2004. *J. Comp. Chem*. 25, 1656–1676.
7. M. Nardini, S. Spano, C. Cericola, A. Pesce, A. Massaro, E. Millo, A. Luini, D. Corda, and M. Bolognesi. 2003. CtBP/BARS: a dual-function protein involved in transcription co-repression and Golgi membrane fission. *EMBO J*. 22, 3122–3130.
8. H. J. C. Berendsen, J. P. M. Postma, W. F. Van Gunsteren, and J. Hermans. Interaction model for water in relation to protein hydration, pages 331-342. D. *Reidel Publishing Company, Dordrecht*, The Netherlands, 1981.
9. T.A. Darden, D.M. York, and L.G. Pedersen. Particle mesh Ewald: ”An Nlog(N) method for Ewald sums in large systens”. 1993. *J. Chem. Phys*. 98, 10089–10092.
10. H.J.C. Berendsen, J.P.M. Postma, W. van Gunsteren, A. Di Nola, and J.R. Haak. 1984. Molecular dynamics with coupling to an external bath. *J. Chem. Phys*. 81, 3684.

Supplementary Figure 1

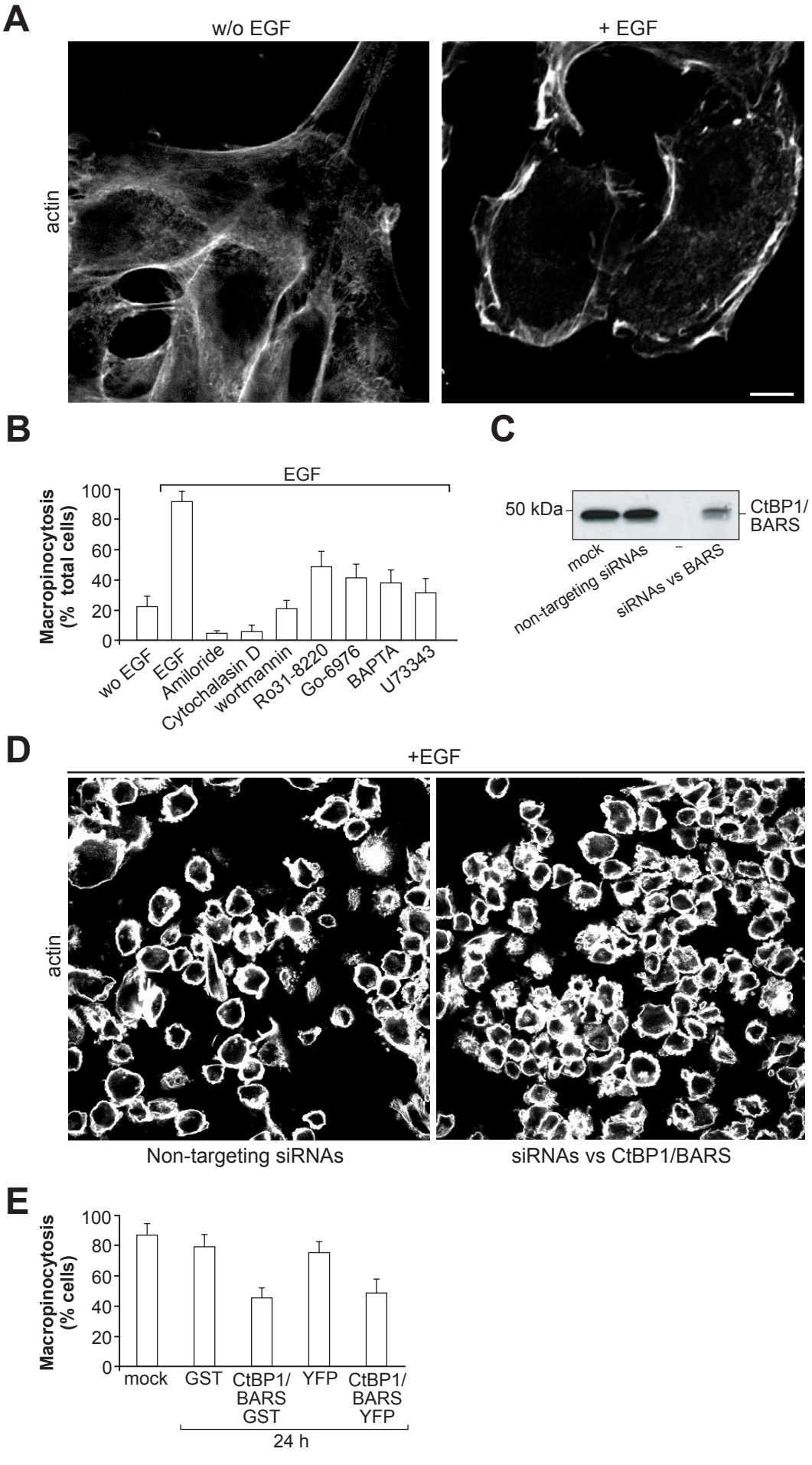

Supplementary Figure 2

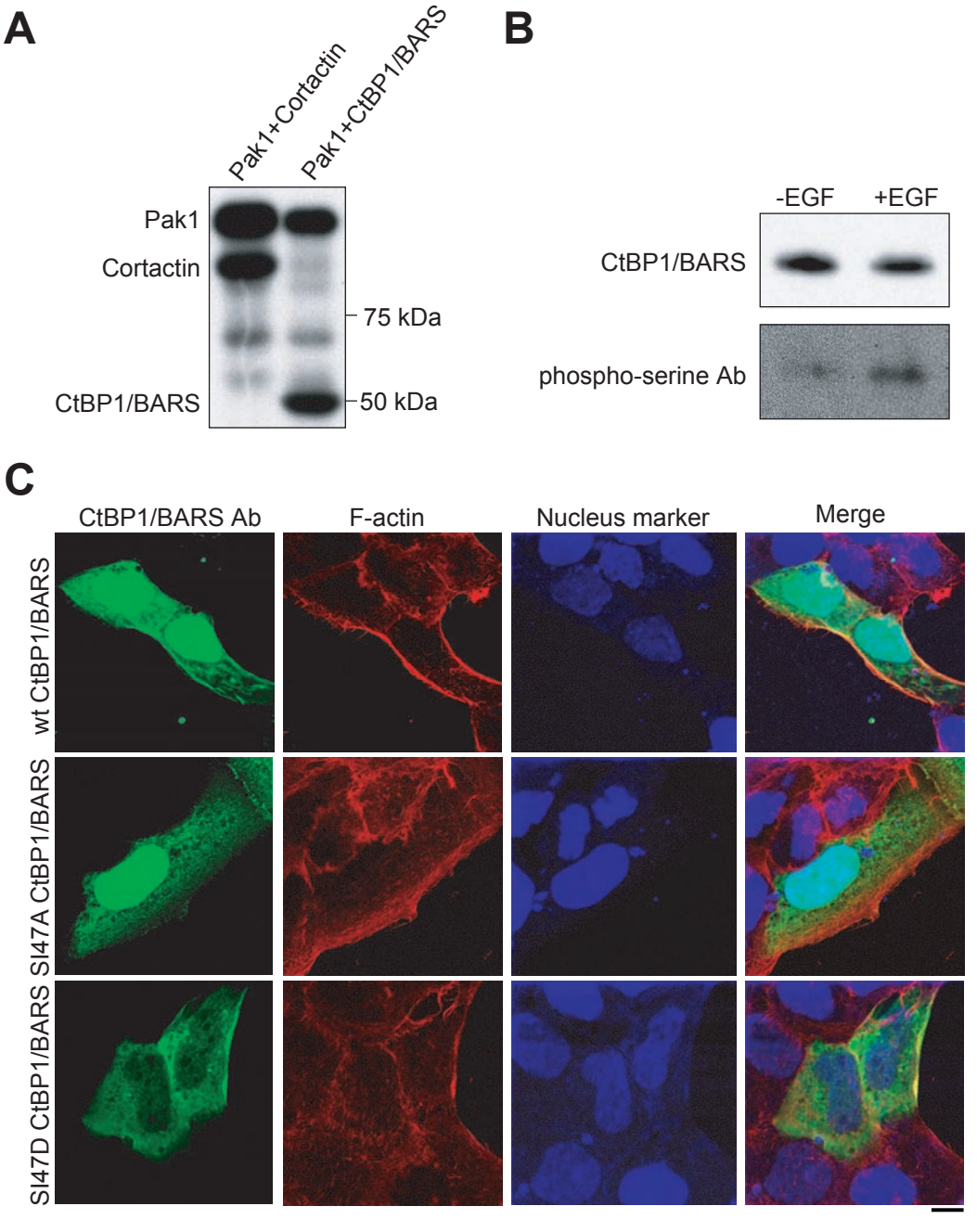

Supplementary Figure 3

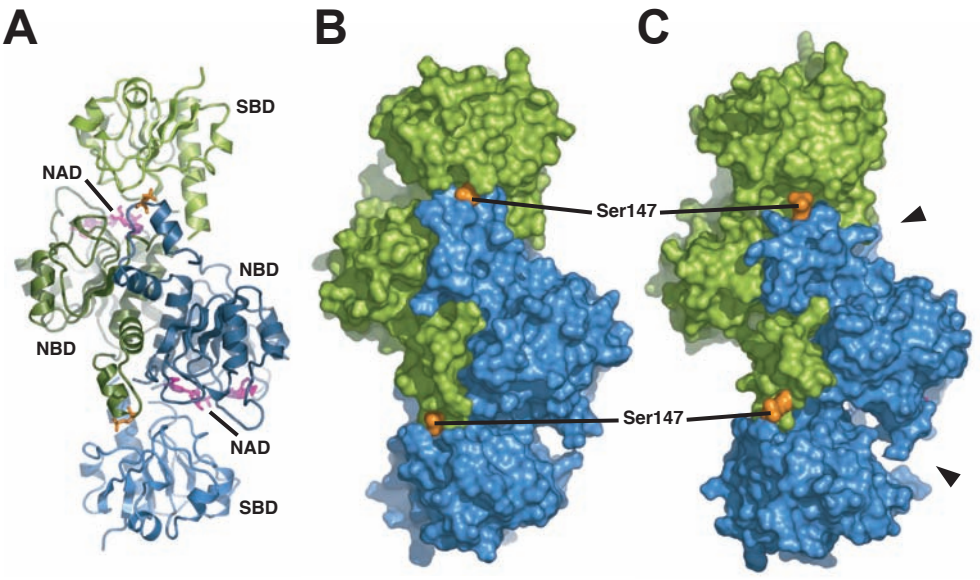

following 10 n sec.
molecular dynamics